MOLECULAR AND CELLULAR BIOLOGY, Nov. 1989, p. 4777–4788
0270-7306/89/114777-12$02.00/0

Vol. 9, No. 11

Photolyases from *Saccharomyces cerevisiae* and *Escherichia coli* Recognize Common Binding Determinants in DNA Containing Pyrimidine Dimers

MARK BAER AND GWENDOLYN B. SANCAR*

Department of Biochemistry, The University of North Carolina at Chapel Hill, Chapel Hill, North Carolina 27599-7260

Received 25 April 1989/Accepted 19 July 1989

DNA photolyases catalyze the light-dependent repair of pyrimidine dimers in DNA. The results of nucleotide sequence analysis and spectroscopic studies demonstrated that photolyases from *Saccharomyces cerevisiae* and *Escherichia coli* share 37% amino acid sequence homology and contain identical chromophores. Do the similarities between these two enzymes extend to their interactions with DNA containing pyrimidine dimers, or does the organization of DNA into nucleosomes in *S. cerevisiae* necessitate alternative or additional recognition determinants? To answer this question, we used chemical and enzymatic techniques to identify the contacts made on DNA by *S. cerevisiae* photolyase when it is bound to a pyrimidine dimer and compared these contacts with those made by *E. coli* photolyase and by a truncated derivative of the yeast enzyme when bound to the same substrate. We found evidence for a common set of interactions between the photolyases and specific phosphates in the backbones of both strands as well as for interactions with bases in both the major and minor grooves of dimer-containing DNA. Superimposed on this common pattern were significant differences in the contributions of specific contacts to the overall binding energy, in the interactions of the enzymes with groups on the complementary strand, and in the extent to which other DNA-binding proteins were excluded from the region around the dimer. These results provide strong evidence both for a conserved dimer-binding motif and for the evolution of new interactions that permit photolyases to also act as accessory proteins in nucleotide excision repair. The locations of the specific contacts made by the yeast enzyme indicate that the mechanism of nucleotide excision repair in this organism involves incision(s) at a distance from the pyrimidine dimer.

Since its initial description in 1949, photoreactivation of UV-induced DNA damage has been characterized in a wide variety of organisms, including bacteria, fungi, plants, invertebrates, and all major groups of vertebrates except placental mammals (for reviews, see references 13, 33, 36, and 48). Enzymatic photoreactivation is carried out by DNA photolyases that bind to *cis-syn* cyclobutane dipyrimidines (pyrimidine dimers) in DNA and subsequently absorb and utilize the energy in a photon of near-UV or visible light to cleave the cyclobutane ring in a reaction that regenerates two intact pyrimidine monomers (26, 27, 42). A variety of in vivo and in vitro studies indicate that DNA photolyases have a number of properties in common: (i) they bind specifically and exclusively to pyrimidine dimers in DNA (13, 48); (ii) they are relatively insensitive to the sequence context in which the dimer is embedded (23, 25, 26); (iii) the enzymes interact with components of the endogenous nucleotide excision repair pathways to increase the efficiency of dimer excision in the dark (14, 30, 37, 54); and (iv) they bind specific cofactors that are the chromophores responsible for absorbing photoreactivating light (36). Nucleotide sequence analyses of the cloned apoenzyme genes from *Escherichia coli*, *Saccharomyces cerevisiae*, and *Anacystis nidulans* suggest that these functional similarities are reflected in the primary structures of the photolyases; the amino acid sequences of these enzymes, predicted from the nucleotide sequences, are 30 to 40% identical with some regions exhibiting greater than 50% identity (35, 39, 55, 56). In addition, all purified photolyases thus far examined contain two chromophores, reduced flavin adenine dinucleotide and either 5,10-methenyltetrahydrofolate (*E. coli* and *S. cerevisiae* [18, 32, 38]) or 8-hydroxy-5-deazaflavin (*A. nidulans*, *Streptomyces griseus*, *Scendesmus acutus*, and *Methanobacterium thermoautotrophicum* [4–6, 19a, 29). To date, neither the DNA-binding domain nor the chromophore-binding sites of any photolyase have been identified, and therefore it is not clear whether the similarities in the primary amino acid sequences of these enzymes reflect conservation of one or several structural and functional domains.

Photolyases recognize pyrimidine dimers in DNA with a selectivity similar to that of sequence-specific DNA-binding proteins (40). Whereas the sequence and composition of pyrimidine dimers can influence the efficiency of binding (23, 44), dimers of thymine or thymidine are not bound to a measurable extent (19, 43), indicating that two pyrimidine nucleotides linked by a cyclobutane ring do not contain sufficient structural information to specify efficient photolyase binding. We have previously mapped some of the contacts made on DNA when *E. coli* photolyase binds to a pyrimidine dimer at a unique location in a defined 43-base-pair (bp) substrate (17). Those studies revealed that the bacterial enzyme contacts a 6- to 7-base region around the dimer, approaches the dimer from the major groove, and makes contact with specific phosphates both 5′ and 3′ to the pyrimidine dimer. Do photolyases from different organisms recognize similar features of the DNA surrounding the dimer? This question is particularly pertinent to photolyases from eucaryotes in which the organization of DNA into nucleosomes may alter the structure of the DNA surrounding the dimer. Studies on the effect of oligonucleotide chain length on repair have suggested that the *E. coli* enzyme recognizes dimers embedded in short oligonucleotides more efficiently than does yeast photolyase (19, 43; G. B. Sancar and F. W. Smith, unpublished observations). In addition, as

* Corresponding author.

is shown in the accompanying work (37), whereas photolyase from yeast can efficiently complement the defect in light-dependent repair in *E. coli phr-1* strains, it inhibits rather than enhances nucleotide excision repair in the bacterium. In this communication, we identify the contacts made on DNA by *S. cerevisiae* photolyase when it is bound to a pyrimidine dimer and compare these contacts with those made by *E. coli* photolyase and by a truncated derivative of the yeast enzyme when bound to the same substrate. Our results indicate that the enzymes recognize a common set of structural determinants in dimer-containing DNA. Superimposed on this common pattern are significant differences in the contributions of specific contacts to the overall binding energy, in the interactions of the enzymes with groups on the complementary strand, and in the extent to which other DNA-binding proteins are excluded from the region around the dimer. We also report several contacts for the *E. coli* enzyme that were not seen in our previous work and that provide a more comprehensive characterization of the interactions at the DNA-protein interface. Together, these results modify our concept of how the enzymes approach and recognize pyrimidine dimers in double-stranded DNA.

MATERIALS AND METHODS

Enzymes and chemicals. Enzymes and chemicals were obtained from the following sources: DNase I (DPRF from Worthington Diagnostics; T4 DNA ligase and T4 polynucleotide kinase, Bethesda Research Laboratories, Inc.; [γ-^{32}P]ATP (7,000 Ci/mmol), Dupont, NEN Research Products; calf thymus DNA, yeast 5S RNA, phosphocellulose, and ethylnitrosourea, Sigma Chemical Co.; and dimethyl sulfate, Eastman Chemical Products, Inc. Methidiumpropyl-EDTA (MPE) was a gift from Peter Dervan, California Institute of Technology. The 11-base oligonucleotide containing a single *cis-syn* pyrimidine dimer was prepared as described previously (1).

Preparation of the 43-bp substrate. The 43-bp substrate containing a single pyrimidine dimer at a defined site and its nondimer counterpart were assembled from six single-stranded synthetic oligonucleotides as described by Husain et al. (17), with the following modifications. The top strand was labeled by incubating 1.5 μg of the top left oligonucleotide with 2 mCi of [γ-^{32}P]ATP and 10 U of T4 kinase in a volume of 30 μl. The ligation mixture contained the labeled top left oligonucleotide, 0.5 μg of the dimer-containing oligonucleotide or its nondimer counterpart, and 3 μg of the five remaining oligonucleotides; ligations were carried out in a volume of 100 μl because we found that smaller volumes reduced the yield of full-length product. Substrate labeled on the bottom strand was constructed similarly. The sequence of the substrate was confirmed by chemical sequencing methods (21) and is shown below, as is the location of the pyrimidine dimer:

```
      1         10        20        30        40
5'-pCTATCGATGGCCTGCAGGCAAGTTGGAGGAATTCGTACTGAGTC-3'
3'   ATAGCTACCGGACGTCCGTTCAACCTCCTTAAGCATGACTCAGT-5'
      1'        10'       20'       30'       40'
```

Photolyases. Yeast photolyase (Phr1) was purified by using our original procedure (38) with modifications that led to separation of Phr1*, a truncated form of Phr1 photolyase, from Phr1. After the first Blue Sepharose CL4B column, photolyase-containing fractions were pooled, dialyzed into phosphocellulose column buffer (0.1 M KCl, 50 mM KPO_4, 1 mM EDTA, 20% glycerol) and applied to a phosphocellulose column (16 by 81 mm) equilibrated in the same buffer. After a 65-ml wash with the same buffer, a 150-ml linear gradient of 0.1 to 0.8 M KCl was applied; Phr1* and Phr1 eluted at 17 and 28%, respectively, of the gradient. Purification was then continued as described previously (38). *E. coli* photolyase was provided by A. Sancar and was purified as previously described (34).

Photolyase-binding reaction and separation of bound and nonbound substrate. Binding reactions were performed at 23°C in a 50-μl reaction mixture containing 50 mM Tris base (pH 7.5), 1 mM EDTA, 100 mM NaCl, 1 mM β-mercaptoethanol, 100 μg of bovine serum albumin per ml, 2 μg of calf thymus DNA, 5 μg of 5SRNA, 25 nM labeled substrate, and photolyase at a concentration of 1 mM unless otherwise noted. Under these conditions, >95% of the substrate was bound as determined by band shift analysis (see below), whereas <5% of oligonucleotide lacking dimer was bound (data not shown). All reactions and subsequent manipulations were performed under General Electric gold fluorescent lamps to prevent uncontrolled photoreactivation. When desired, photoreactivating light was administered via the simultaneous discharge of two Vivitar model 283 photographic flash units.

Photolyase-bound complexes were separated from nonbound DNA by the band shift technique (9, 11, 16). After addition of glycerol to 6%, the reaction mixtures were loaded onto 8% polyacrylamide gels (16 cm long by 1.5 mm thick) in TBE buffer (90 mM Tris base, 90 mM boric acid, 2.5 mM EDTA) and electrophoresed at 30 to 35 mA for 90 min, at which time the nonbound substrate had migrated two-thirds of the distance from the top of the gel. The gels were then autoradiographed, and the separated bands were sliced from the gel and placed in 1.5-ml microfuge tubes. Elution buffer (400 μl; 1.5% SDS, 0.5 M ammonium acetate, 100 mM Tris hydrochloride [pH 7.5], 1 mM EDTA) was added to each tube, which was then agitated continuously at 37°C for at least 4 h. The gel slice was removed, and the DNA was precipitated by addition of 1 ml of 95% ethanol.

Preliminary experiments indicated that the yeast and *E. coli* photolyase footprints were best compared by performing the binding reactions simultaneously and analyzing the reaction products in parallel. Thus, for each procedure described below, Phr1, Phr1*, and *E. coli* photolyases were used in parallel and with the same preparation of modified substrate. Each footprinting experiment was performed at least twice.

MPE-Fe(II) footprinting. The binding reaction was performed with photolyases at a concentration of 0.2 mM. MPE-Fe(II) footprinting was carried out as described previously by Husain et al. (17) except that the concentration of MPE-FeII was doubled and the reaction time was reduced to 10 min. These conditions yielded clearer footprints than those obtained in our previous work.

DNase I footprinting. The photolyase-binding reaction was performed as described above except that a photolyase concentration of 2 mM was used. After binding, $MgCl_2$ (10 mM), $CaCl_2$ (8 mM), and 0.013 U of DNase I were added; 3 min later, the reaction was terminated by addition of EDTA to a final concentration of 20 mM. The samples were lyophilized and suspended in 40 μl of formamide-dye mixture (1 mM EDTA, 0.1% [wt/vol] xylene cyanol, 0.1% [wt/vol] bromophenol blue, 80% deionized formamide).

Ethylation interference. DNA was treated with ethylnitrosourea (ENU) as described by Siebenlist and Gilbert (45). Carrier RNA (25 μg) was then added, and the DNA was precipitated in ethanol seven times to remove all traces of ENU. The photolyase-binding reaction was then performed,

and bound and nonbound DNAs were separated. Before elution of the DNA from the gel, the samples were exposed to photoreactivating light. This latter step was necessary to assess the effect of ethylation of the intradimer phosphate on binding; in the absence of photoreactivation, phosphodiester bond cleavage at this site will not be apparent because the cyclobutane ring links the two portions of the DNA strand. Strand cleavage was performed as described previously (45).

Methylation protection and methylation interference. Methylation protection and interference reactions were carried out as described by Husain et al. (17) except that bound and nonbound complexes were separated on acrylamide gels as described above.

Missing-contact assay. DNA was modified as described by Brunelle and Schleif (3) except that after base cleavage, the DNA was precipitated with 95% ethanol. Modified substrate was then used in the photolyase-binding reaction, and bound and nonbound complexes were separated. Piperidine-induced strand cleavage was performed as described by Maxam and Gilbert (21).

Product analysis. Products from the footprinting reactions were heated in formamide-dye mixture at 90°C for 2 min and then analyzed on 12% DNA sequencing gels in 2× TBE buffer (17). Electrophoresis was discontinued when the bromophenol blue dye reached the bottom. The gels were dried and subjected to autoradiography, using Kodak XAR-5 film and Cronex Lightning-Plus intensifying screens. Quantitative analyses were carried out by using either a Biomed Instruments scanning laser densitometer (for protein gels and autoradiographs) or an Ambis radioanalytic imaging system (for sequencing gels).

RESULTS

Separation of full-length and truncated photolyase. We have previously reported purification of the *S. cerevisiae* Phr1 photolyase from a genetically engineered *E. coli* strain (38). In the final preparation, two major bands were seen on sodium dodecyl sulfate-polyacrylamide gels, corresponding to full-length Phr1 photolyase and to Phr1*, a truncated form of Phr1 that is missing 15 to 20 amino acids, probably from the carboxy terminus (38). Studies on preparations containing either 80% Phr1 or 75% Phr1* failed to detect any difference in the absorbance spectra of the two proteins or in the molar ratio of chromophore to apoprotein for either the flavin or folate chromophore (Sancar and Smith, unpublished observations), suggesting that the truncation creating Phr1* does not affect chromophore binding; in addition, repair activities measured under conditions of protein turnover were similar for Phr1 and Phr1*. To further explore the possibility that truncation affects binding of photolyase to the pyrimidine dimer, we compared the footprint obtained with photolyase preparations containing 75% Phr1 and 25% Phr1* with that obtained with an essentially pure preparation of Phr1* (Fig. 1), obtained as described in Materials and Methods.

Determination of the MPE-FeII footprints of the photolyases. For all of the experiments described below, the substrate was a 43-bp oligonucleotide containing a single pyrimidine dimer at a unique location. We used MPE-FeII as a probe to define the limits of the DNA-protein interface when Phr1, Phr1*, and *E. coli* photolyase are bound to the substrate. MPE-FeII intercalates between bases in double-stranded DNA via the methidium moiety and, in the presence of oxygen, attacks the first or second deoxyribose 3′ to the intercalation site, resulting in strand cleavage accompanied by base elimination (15). Because MPE-FeII is small and both intercalation and strand cleavage are relatively insensitive to sequence context, footprints obtained by using this reagent more accurately reflect the size and location of protein and small ligand-binding sites than do footprints obtained by using nucleases as probes (50).

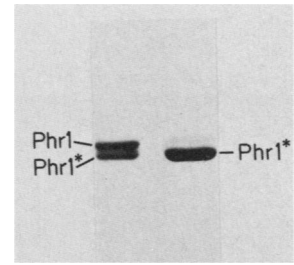

FIG. 1. Purity of the Phr1 and Phr1* preparations used for footprinting. Shown is a photograph of a Coomassie-blue stained sodium dodecyl sulfate-polyacrylamide gel (38) containing samples from the final purified fractions of Phr1 and Phr1*. Each lane contained 6 μg of protein. Only the bands shown in the photograph were visible on the gel.

The MPE-FeII footprints obtained with the three enzymes on the 43-bp unique dimer substrate were essentially identical (Fig. 2). Each enzyme protected regions of 6 to 7 bp on the top strand and 7 to 8 bp on the bottom strand, and the protected residues were symmetrically disposed around the pyrimidine dimer. (In the dimer-containing DNA, the band corresponding to the intradimer phosphodiester bond is missing because the cyclobutane ring links the strand cleavage products). Two controls demonstrated that the observed footprints were due specifically to binding by the photolyases: (i) the footprints were absent when the purified enzymes were incubated with nondimer substrate, indicating that a pyrimidine dimer is required, and (ii) application of a single flash of photoreactivating light to the photolyase-dimer complexes before addition of MPE-FeII resulted in loss of the footprint and the appearance of an MPE-FeII cleavage pattern identical to that seen with the nondimer substrate.

Identification of phosphate contacts. DNA phosphates interacting with or in close proximity to bound photolyases were identified by the ethylation interference technique in which ENU was used to alkylate phosphates in the DNA backbone (45). When photolyase is incubated with ethylated dimer-containing DNA, the enzyme fails to bind molecules in which crucial ionic contacts are eliminated by alkylation or in which addition of the bulky ethyl group interferes sterically with binding (45, 46). Molecules that are not bound by the enzyme can be separated from bound molecules by electrophoresis through polyacrylamide gels, and the specific modified phosphates in each fraction can be revealed by base-induced strand cleavage at the ethylated phosphates. The results of such an experiment using Phr1, Phr1*, and *E. coli* photolyase are shown in Fig. 3. On the dimer-containing strand (Fig. 3A), ethylation of the phosphate immediately 5′ to the dimer, as well as the first through the third phosphates 3′ to the dimer, inhibited binding by Phr1 and Phr1* (lanes 2 versus 3 and 5 versus 6); the pattern obtained with *E. coli* photolyase was qualitatively similar except that ethylation at the fourth phosphate 3′ to the dimer also inhibited binding, albeit weakly (lanes 9 and 10). As we have noted previously for the *E. coli* enzyme (17), ethylation of the phosphodiester bond between the two T's in the dimer does not inhibit

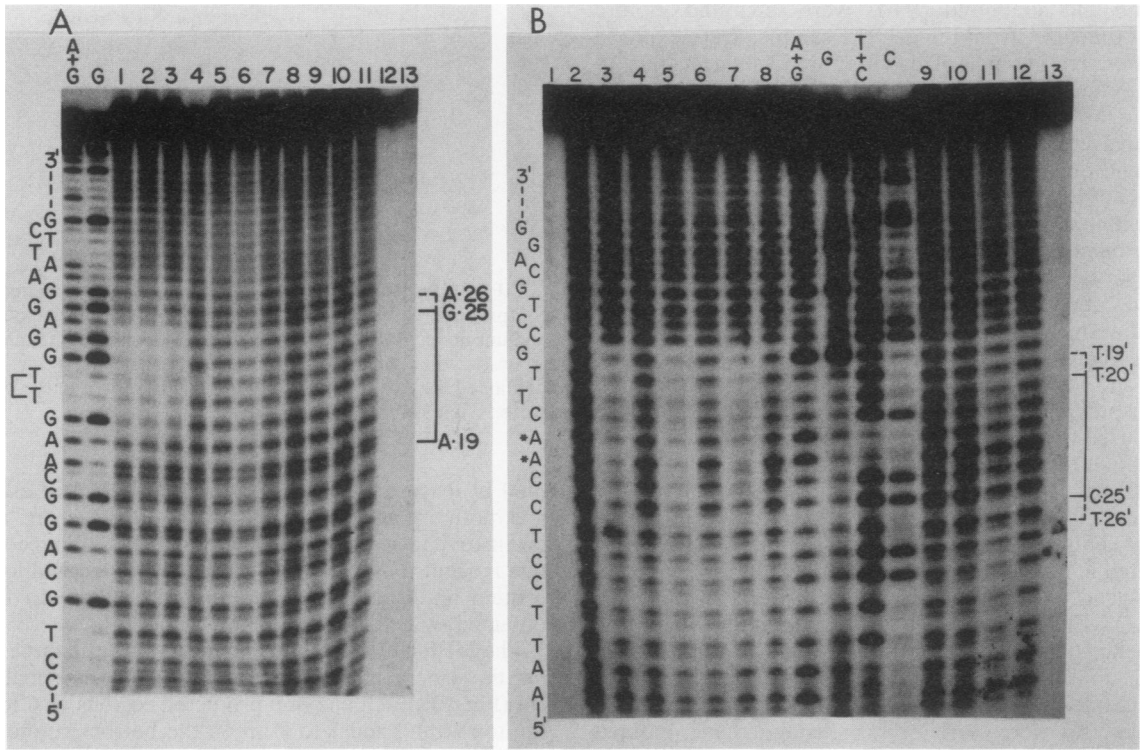

FIG. 2. Determination of photolyase-DNA contacts by MPE-FeII footprinting. The unique dimer substrate, or the analogous substrate without a dimer, was incubated with MPE-FeII in the presence or absence of the various photolyases, and the products were analyzed on DNA sequencing gels in parallel with the Maxam-Gilbert sequencing products (21) from the nondimer substrate (lanes A + G, G, T + C, and C). The sequence is shown to the left in both panels, and the numbering is as given in Materials and Methods. The bracket on the right indicates protected phosphodiester bonds, taking into account the fact that the MPE-FeII footprint is shifted 1 to 2 bp 3′ to the actual binding site (15, 50); dashed regions of the bracket indicate partial protection. (A) Footprint on the top strand. The bracketed T's on the left indicate the pyrimidine dimer. Lanes 1 to 7 and 13 contain unique dimer substrate treated as follows: 1, incubated with MPE-FeII after incubation with Phr1; 2, as lane 1 except with Phr1*; 3, as lane 1 except with *E. coli* photolyase; 4, incubated with MPE-FeII only; 5 to 7, as lanes 1 to 3 except that the photolyase-substrate complexes were exposed to photoreactivating light before addition of MPE-FeII; 13, substrate alone, not treated with MPE-FeII. Lanes 8 to 12 contain nondimer substrate treated as follows: 8, incubated with MPE-FeII only; 9 to 11, incubated with Phr1, Phr1*, and *E. coli* photolyase, respectively, before addition of MPE-FeII; 12, nondimer DNA alone, not treated with MPE-FeII. (B) Footprint on the bottom strand. The starred A's indicate the bases opposite the dimer. Lanes 1 to 8 contain unique dimer substrate; lanes 9 to 13 contain nondimer substrate. Lanes: 1, untreated substrate; 2, substrate treated with MPE-Fe(II) only; 3, substrate incubated with Phr1 before addition of MPE-FeII; 4, as lane 3 except that the Phr1-substrate complexes were exposed to photoreactivating light before addition of MPE-Fe(II); 5 and 6, same as lanes 3 and 4 except with Phr1 photolyase; 7 and 8, same as lanes 3 and 4 except with *E. coli* photolyase; 9, nondimer DNA treated with MPE-Fe(II) only; 10, nondimer DNA incubated with Phr1 before addition of MPE-Fe(II); 11 and 12, same as lane 10 except with Phr1* and *E. coli* photolyase, respectively; 13, untreated nondimer DNA.

binding. On the complementary strand (Fig. 3B), modification of the phosphate between $T_{19'}$ and $G_{18'}$ reduced binding by each of the three photolyases (lanes 2 versus 3, 7 versus 8, and 11 versus 12). This phosphate lies immediately across the minor groove from the 5′ and intradimer phosphodiester bonds. In our previous report on the footprint of the *E. coli* enzyme, we did not detect this relatively weak contact (17), probably because the nitrocellulose filters used to separate bound from nonbound substrate did not retain the *E. coli* photolyase-DNA complexes efficiently (41). This finding demonstrates the superiority of the band shift technique for DNA-protein complexes that are not retained efficiently on nitrocellulose filters.

Despite the qualitative similarity in the number and locations of modified phosphates that inhibit binding, ethylation at specific phosphates has different quantitative effects on the binding equilibria of the yeast and *E. coli* enzymes, as evidenced by the different degrees of binding inhibition. Modification of the first or second phosphates 3′ to the dimer almost completely eliminated binding by both enzymes, whereas modification of the first phosphate 5′ to the dimer or the third phosphate 3′ to the dimer greatly diminished *E. coli* photolyase binding but only moderately inhibited binding by Phr1 and Phr1*. These results are consistent with a model whereby the yeast enzyme utilizes ionic interactions primarily with the first and second phosphates 3′ to the dimer as important binding determinants. Although it is clear that these interactions are also important for *E. coli* photolyase binding, the latter enzyme also interacted strongly with, or is nearer to, additional phosphates on both sides of the dimer. In addition, ethylation of the phosphate between $T_{19'}$ and $G_{18'}$ interfered more with binding by Phr1 and Phr1* than with binding by the *E. coli* enzyme, suggesting that the yeast enzyme lies closer to this residue.

Identification of major and minor groove contacts. Treatment of double-stranded DNA with dimethyl sulfate (DMS) results in preferential methylation of N7 of guanine and N3 of adenine, which lie, respectively, in the major and minor grooves of DNA. These atoms can be protected from methylation when hydrogen bonded to or in close proximity to a

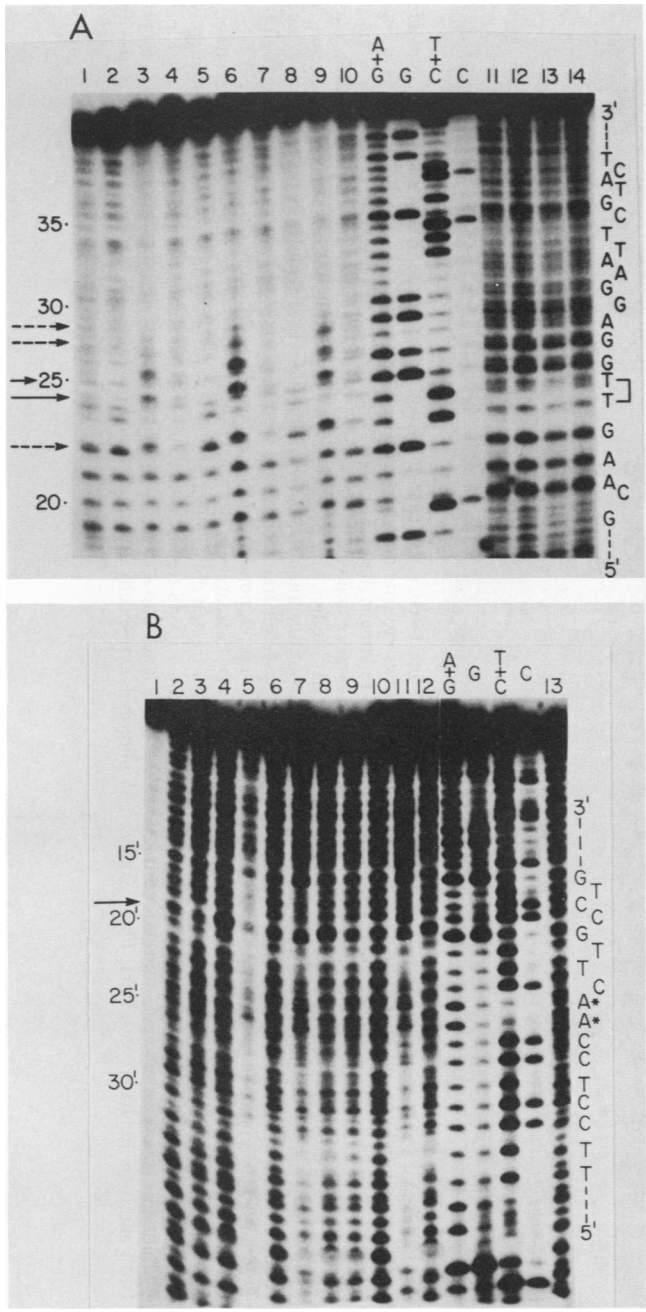

FIG. 3. Determination of sites at which phosphate modification interferes with photolyase binding. Dimer and nondimer substrate were treated with ENU and incubated with photolyase; then bound and nonbound substrates were separated on the basis of retardation in polyacrylamide gels and analyzed as described in Materials and Methods. Arrows indicate phosphodiester bonds at which ethylation inhibits photolyase binding as shown by increased relative intensity of a band in the nonretarded fraction; the dashed arrows indicate positions at which modification appeared to interfere more with binding by *E. coli* photolyase than with binding by yeast photolyase. Sequence and numbering are as in Fig. 2. (A) Analysis of the top strand. Bracketed T's indicate the dimer. Lanes 1 to 10 contain the unique dimer substrate treated with ENU; lanes 11 to 14 contain analogous nondimer DNA. Lanes: 1, ENU-treated substrate without photolyase; 2, substrate incubated with Phr1 after ENU treatment, retarded fraction; 3, as lane 2 except nonretarded fraction; 4, Phr1-substrate complexes exposed to photoreactivating light before separation on acrylamide gels, nonretarded fraction; 5 to 7, same as lanes 2 to 4 except with Phr1*; 8 to 10, same as lanes 2 to 4 except with *E. coli* photolyase; 11, ENU-treated nondimer DNA without photolyase; 12 to 14, nonretarded fractions from reactions containing Phr1, Phr1*, and *E. coli* photolyase, respectively. (B) Analysis of the bottom strand. Starred A's indicate the bases opposite the dimer. Lane 1, Unique dimer substrate not exposed to enzyme or to ENU. Lanes 2 to 12 contain dimer substrate exposed to ENU and then treated as follows: 2, no enzyme; 3, incubated with Phr1 after ENU treatment, retarded fraction; 4, as lane 3 except nonretarded fraction; 5, Phr1-substrate complexes exposed to photoreactivating light before separation on an acrylamide gel, retarded fraction; 6, as lane 5 except nonretarded fraction; 7 to 10, as lanes 3 to 6 except with Phr1*; 11 and 12, as lanes 3 and 4 except with *E. coli* photolyase; 13, ENU-treated nondimer DNA.

DNA-binding protein, and methylation before addition of the protein can inhibit binding either by elimination of essential hydrogen bonds or by steric hindrance. Figure 4 shows the results of methylation protection and interference experiments designed to identify major and minor groove contacts and to determine which contacts are required for photolyase binding. Overall, the methylation effects were quite small; for this reason, autoradiographs of all lanes were scanned and the intensities were normalized relative to those of bands not affected by the presence of the photolyases (data not shown). Comparison of the methylation patterns obtained when the unique dimer substrate or photolyase-DNA complexes were exposed to DMS revealed modest protection by the enzymes of the first G 5′ to the dimer (G_{21}; Fig. 4A, lanes 2, 3, and 5). In addition, Phr1 also protected the second G 3′ to the dimer (G_{25}). An identical pattern was observed for Phr1*-DNA complexes (data not shown). In contrast to our previous study, we did not observe weak protection of G_{25} by *E. coli* photolyase; the reason for this difference is not clear. On the complementary strand (Fig. 4B), binding of yeast photolyase protected both A's opposite the dimer ($A_{22'}$ and $A_{23'}$; lanes 2 and 3) from methylation, whereas *E. coli* photolyase failed to protect any base but rather enhanced methylation of $A_{22'}$ opposite the 5′ T in the dimer (lanes 6 and 7). When DNA was methylated and exposed to photolyase and the bound and nonbound complexes were separated (Fig. 4C), modification at G_{21} and G_{25} inhibited binding by all three photolyases (lanes 2 versus 3, 5 versus 6, and 8 versus 9); however, the relative degree of inhibition differed both between sites and between enzymes, with methylation at G_{25} producing the greatest inhibition in all cases. Methylation at G_{21} had somewhat greater effect on binding by *E. coli* photolyase than on binding by the yeast enzyme (lanes 2 versus 3 and 8 versus 9). In addition, methylation of G_{24}, the first G 3′ to the dimer, enhanced binding by *E. coli* photolyase (lanes 8 versus 9) but had no effect on binding by yeast photolyase (lanes 2 versus 3 and 5 versus 6). No interference due to methylation was seen on the complement to the dimer-containing strand (data not shown).

Because photolyases repair pyrimidine dimers in a variety of sequence contexts (23, 25), the contacts revealed by methylation protection and interference probably are not required hydrogen-bonding sites, as is the case for sequence-specific DNA-binding proteins, but rather reflect close approach of the proteins to the reactive nitrogens. Therefore, we conclude that portions of the photolyases lie in the major groove of DNA both 5′ and 3′ to the dimer. The observed effects on methylation of the A's complementary to the dimer suggest that portions of these enzymes may also lie in the minor groove. The N3 atoms on $A_{22'}$ and $A_{23'}$ are

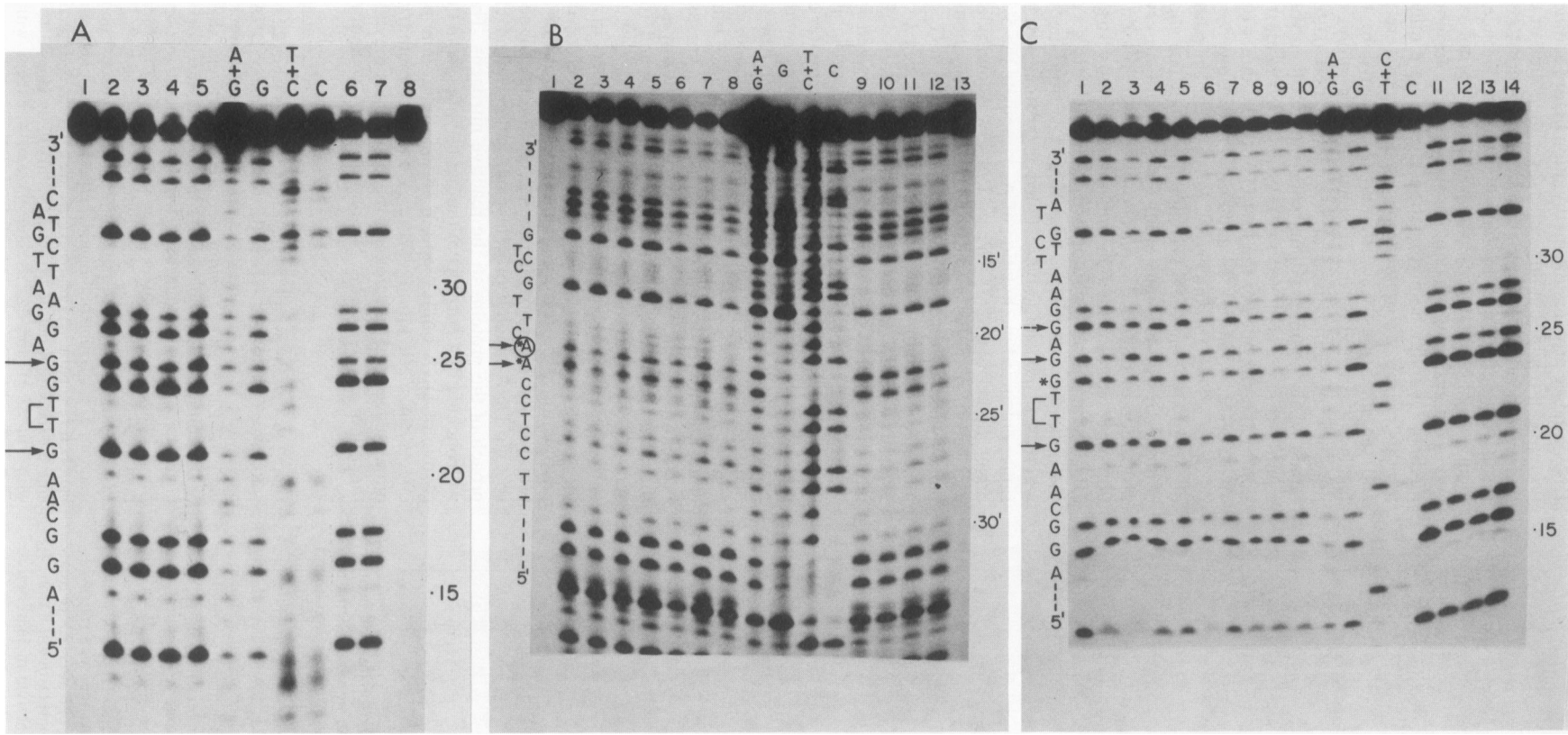

FIG. 4. Major and minor groove contacts made by photolyase as determined by methylation protection and interference. Bracketed T's indicate the dimer, and starred A's indicate the position opposite the dimer. Arrows indicate positions of methylation interference or protection; dashed arrows indicate marginal responses. Sequence and numbering are as in Fig. 2. (A) Methylation protection analysis of the top strand. Lanes: 1 and 2, unique dimer substrate without DMS treatment (lane 1) or with DMS treatment only (lane 2); 3, unique dimer substrate incubated with Phr1 then exposed to DMS; 4, as lane 3 except that the substrate-photolyase complexes were exposed to photoreactivating light before addition of DMS; 5, as lane 3 except with *E. coli* photolyase; 6 to 8, as lanes 2, 3, and 1, respectively, except with nondimer DNA. (B) Methylation protection analysis of the bottom strand. The circled A indicates the position of methylation enhancement seen with *E. coli* photolyase. Lanes: 1 and 2, unique dimer substrate without DMS treatment (lane 1) or with DMS treatment only (lane 2); 3, unique dimer substrate incubated with Phr1 and then exposed to DMS; 4, as lane 3 except that the photolyase-substrate complexes were exposed to photoreactivating light before addition of DMS; 5 and 6, as lanes 3 and 4 except with Phr1*; 7 and 8, as lanes 3 and 4 except with *E. coli* photolyase; 9, nondimer DNA exposed to DMS only; 10 to 12, nondimer DNA exposed to DMS after addition of Phr1, Phr1*, and *E. coli* photolyase, respectively; 13, nondimer DNA without DMS treatment. (C) Methylation interference analysis of the top strand. The starred G indicates the position at which methylation enhanced binding by *E. coli* photolyase. Lanes: 1, DMS-treated dimer substrate; 2, DMS-treated dimer substrate subsequently incubated with Phr1, retarded fraction; 3, DMS-treated dimer substrate incubated with Phr1, nonretarded fraction; 4, DMS-treated dimer substrate subsequently incubated with Phr1 and then exposed to photoreactivating light before separation on an acrylamide gel, nonretarded fraction; 5 to 10, as lanes 2 to 4 except with Phr1* (lanes 5 to 7) or *E. coli* photolyase (lanes 8 to 10); 11 to 13, nondimer DNA treated with DMS and then incubated with Phr1, Phr1*, and *E. coli* photolyase, respectively, nonretarded fractions; 14, nondimer DNA treated with DMS only.

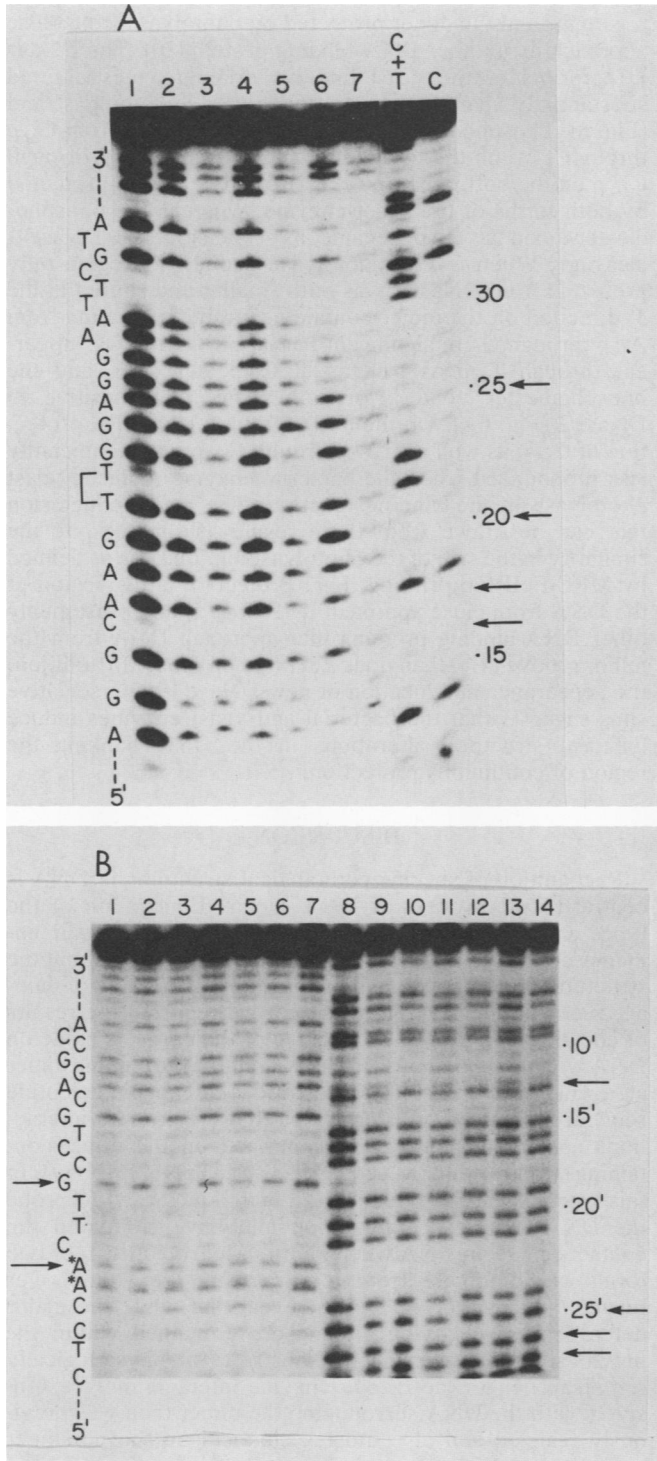

FIG. 5. Missing-contact analysis of the photolyase-DNA interaction. The substrate was subjected to limited depurination or depyrimidination reactions and incubated with one of the photolyases; then the bound and nonbound fractions were separated on the basis of retardation in polyacrylamide gels and analyzed as described in Materials and Methods. Bracketed T's indicate the dimer, and starred A's indicate the position opposite the dimer. Arrows indicate positions at which base removal inhibited photolyase binding. Sequence and numbering are as in Fig. 2. (A) Top strand, effect of A and G removal. Lanes 1 to 7 contain partially depurinated unique dimer substrate. Lanes: 1, substrate only; 2, substrate incubated with Phr1 after depurination, retarded fraction; 3, substrate incubated with Phr1 after depurination, nonretarded fraction; 4 to 7, as lanes 2 and 3 except incubated with Phr1* (lanes 4 and 5) or *E. coli* photolyase (lanes 6 and 7). (B) Bottom strand, effect of A and G removal (lanes 1 to 7) or C and T removal (lanes 8 to 14). Lanes: 1, depurinated DNA incubated with Phr1, retarded fraction; 2, depurinated DNA incubated with Phr1, nonretarded fraction; 3 to 6, as lanes 1 and 2 except with Phr1* (lanes 3 and 4) and *E. coli* photolyase (lanes 5 and 6); 7, depurinated substrate only; 8, depyrimidinated substrate only; 9 to 14, as lanes 1 to 6 except with depyrimidinated substrate.

situated beneath and across the minor groove from the crucial phosphate contacts 3′ to the dimer (see Fig. 7) and thus appear to be appropriately positioned to interact with the enzymes. Alternatively, the methylation effects at these residues may reflect alterations in the helix geometry induced by photolyase binding. It has been proposed that in dimer-containing DNA, the double helix is bent into the major groove and that this bend is accompanied by an increase in the accessibility of the complementary bases to small molecules (24). Photolyase could affect methylation by either increasing or decreasing the bend. The different effects of the yeast and bacterial enzymes on methylation at $A_{22'}$ and $A_{23'}$ suggest that different amino acid residues are in close proximity to the A's, that the enzymes induce different structural alterations in the DNA upon binding, or both.

Missing-contact probing of the photolyase-DNA interaction. Partial depurination or depyrimidination of DNA has been used to identify specific base contacts required for binding by sequence-specific DNA-binding proteins (3). As a first approximation, the binding of photolyase to dimer-containing DNA is not expected to be sequence specific except for the requirement for the pyrimidines in the dimer. However, removal of specific bases might inhibit photolyase binding by eliminating potential sites for base-amino acid stacking interactions, decreasing vertical base stacking, or altering the bond torsion angles within and surrounding the abasic sugar (28). In the vicinity of the dimer, base loss might be expected to relieve the distortion of the sugar-phosphate backbone imposed by the dimer. Therefore, the unique dimer substrate was exposed to conditions leading to limited removal of purine or pyrimidine bases and mixed with the photolyases, and the bound and nonbound fractions were separated and treated with piperidine to cleave the DNA at the site of the missing base. Because the total number of counts loaded per lane was not identical in all cases, autoradiographs of these gels were scanned, and the intensities of several bands that appeared unaffected by photolyase binding were used as standards of comparison to determine whether a particular band was enhanced or diminished relative to the unaffected bands (data not shown).

Removal of the second base 3′ to the dimer (G_{25}) strongly inhibited binding by all three photolyases (Fig. 5A). This base was shown by methylation protection and interference to lie close to the bound enzymes and to be flanked by phosphates implicated in binding in the ethylation interference experiments; therefore, interaction with the base and/or sugar-phosphate backbone at this site is a major determinant of photolyase binding. Similarly, removal of base $G_{18'}$ (Fig. 5B) or its base-pair partner C_{18} (data not shown) resulted in significant loss of binding. $G_{18'}$ lies adjacent to the single phosphate contact identified on the nondimer strand; since we did not observe any methylation effects at this site, we believe that the enzymes either approach $G_{18'}$ from the minor groove or interact with the sugar-phosphate backbone at the edge of the minor groove. Removal of bases A_{20}, G_{17},

and G_{16} (Fig. 5A) and bases $C_{13'}$, $C_{25'}$, $T_{26'}$, and $C_{27'}$ (Fig. 5B) caused moderate reduction in binding. With the exception of $C_{13'}$, all of these bases lie adjacent to or within regions in which the phosphodiester backbone is protected from attack by MPE-FeII or DNase I (see below); although inhibition due to base removal at these sites was relatively small, suggesting that interaction with these bases or with deoxyribose stabilizes binding but is not critical to recognition, these observations indicate that photolyase interacts with a greater region of the DNA than was previously thought (17). In several cases, base loss affected only the yeast or the bacterial photolyase. Removal of base $A_{22'}$ (the A opposite the first T in the dimer) inhibited binding of Phr1 and Phr1* but not of *E. coli* photolyase (Fig. 5B, lanes 1 versus 2, 3 versus 4, and 5 versus 6). As noted above, methylation of this residue was inhibited when the yeast enzyme was bound, but prior methylation of $A_{22'}$ did not inhibit photolyase binding. Together, these results suggest that yeast photolyase approaches $A_{22'}$ from the minor groove and interacts with the base or attached sugar. Loss of bases A_{19} and A_{15} inhibited binding by the bacterial enzyme only (Fig. 5A). The effect at A_{19} was particularly intriguing, since this base is adjacent to the phosphodiester bond cleaved by *E. coli* ABC excision nuclease 5′ to the dimer (31), and cleavage at certain pyrimidine dimers by this repair enzyme is enhanced when *E. coli* photolyase is bound (23, 30). This is the first direct evidence that the two bacterial enzymes lie close to one another at the 5′ incision site.

The results shown in Fig. 5 also indicate that the photolyases can bind efficiently to substrate molecules in which one of the glycosylic bonds in the dimer has been ruptured. Because of the increased acid lability of the glycosylic bonds linking the dimerized pyrimidine bases to deoxyribose (8), the limited acid treatment used to obtain partly depurinated substrate also produced a mixed thymine-thymidylate or thymidylate-thymine dimer that remained attached to the sugar-phosphate backbone of the oligonucleotide via a single glycosylic bond. Cleavage of the glycosylic bond at T_{22} (the 5′ T in the dimer) did not detectably inhibit binding of Phr1 or Phr1* and only slightly inhibited binding by *E. coli* photolyase (Fig. 5A). (T_{23} is much more resistant to acid hydrolysis, and therefore we cannot draw any firm conclusions about its contribution to binding). This is a somewhat surprising result, since cleavage of the glycosylic bond might be expected to relieve the dimer-specific distortion of the phosphodiester backbone as well as alter the puckering of the cyclobutane ring (28). However, it should be noted that considerable deformation of double-stranded DNA is still possible if the energetically favored new conformation maintains hydrogen bonding between both T's in the dimer and the A's on the complementary strand. In addition, we wish to stress that these results do not indicate that binding of the photolyases is insensitive to cleavage of the glycosylic bond, but rather that the decrease in the binding equilibrium is too small to be detected under the conditions used in these experiments; we estimate that the equilibrium association constant decreases by less than an order of magnitude.

DNAse I footprint of photolyases. The footprinting experiments described above identified some of the contacts and DNA structural elements important for photolyase binding and the extent of close contact between DNA and photolyase at the DNA-protein interface. In vivo photolyases must interact with DNA in nucleoprotein complexes, and as is demonstrated in the accompanying paper (37), these interactions can significantly influence the efficiency of repair. We have used DNase I as an enzymatic probe to define the region around the dimer protected by photolyase from close approach by another DNA-binding protein (10). The DNase I footprints of the yeast and bacterial enzymes differed substantially, particularly on the dimer-containing strand (Fig. 6). Phosphodiester bonds within the region from $G_{16}p$ through $T_{31}p$ on the top strand (Fig. 6A) and $T_{29'}p$ through $C_{16'}p$ on the bottom strand (Fig. 6B) were clearly protected by both forms of the yeast enzyme, whereas the phosphodiester bond at $C_{11}p$ became hypersensitive to DNase I cleavage. When *E. coli* photolyase bound, the region fully protected from DNase I was both smaller and shifted in the 3′ direction on the dimer-containing strand, extending from $A_{19}p$ through $G_{28}p$; significant partial protection was apparent through $T_{35}p$ as well as at $C_{11}p$ and $T_{12}p$, and the phosphodiester bond at $A_{29}p$ became hypersensitive to DNase I (Fig. 6A). On the bottom strand (Fig. 6B), protection of $C_{16'}p$ as well as $C_{25'}p$ through $C_{27'}p$ was significantly less pronounced when the bacterial enzyme replaced yeast photolyase in the binding reaction. The major conclusion that can be drawn from these results is that despite the similarity in the size of the photolyase-binding site as defined by MPE-FeII footprinting, Phr1 protects a larger region of the DNA from close approach by DNase I, and presumably other DNA-binding proteins that approach DNA from the minor groove (47), than does *E. coli* photolyase. In addition, the appearance and location of new DNase I-hypersensitive sites suggests that the bacterial and yeast enzymes induce different structural alterations in the DNA flanking the region of continuous protection.

DISCUSSION

Recognition of specific pathological structures in DNA is central to the process of DNA repair. Elucidation of the types and locations of contacts made by DNA repair enzymes on their substrates may provide information about the structural determinants exploited during the course of damage recognition. Several years ago, we reported the results of chemical and enzymatic probing of the contacts made on DNA when *E. coli* photolyase is bound to a pyrimidine dimer at a unique location in a substrate of defined nucleotide sequence. Those results suggested that the primary interactions specifying binding are contained on the dimer-containing strand within the sequence 5′-pTpTpNpNp-3′ (17). In this work, we have extended the techniques used to probe the DNA-photolyase interaction and have compared the contacts made on DNA when photolyase from *E. coli* or two forms of photolyase from *S. cerevisiae* are bound. Our results (summarized in Fig. 7) reveal that while the major determinants specifying binding are contained within the previously defined region, in substrates of physiologically significant length the *E. coli* enzyme interacts more extensively with the DNA surrounding the dimer than was previously realized and also utilizes contacts on the nondimer strand to stabilize the enzyme-substrate complex. In addition, we find that the locations of most of the contacts around the dimer made by yeast photolyase are remarkably similar to those made by the bacterial enzyme, the primary difference being that the yeast enzyme interacts more extensively with the nondimer strand. Both intact Phr1 and Phr1* gave identical footprints in all experiments. These results provide strong evidence for both a core set of recognition contacts used by photolyases to identify dimer-containing DNA as substrate and, within and surrounding this core, a set of interactions that stabilize binding and may also reflect the constraints imposed by the presence of other DNA

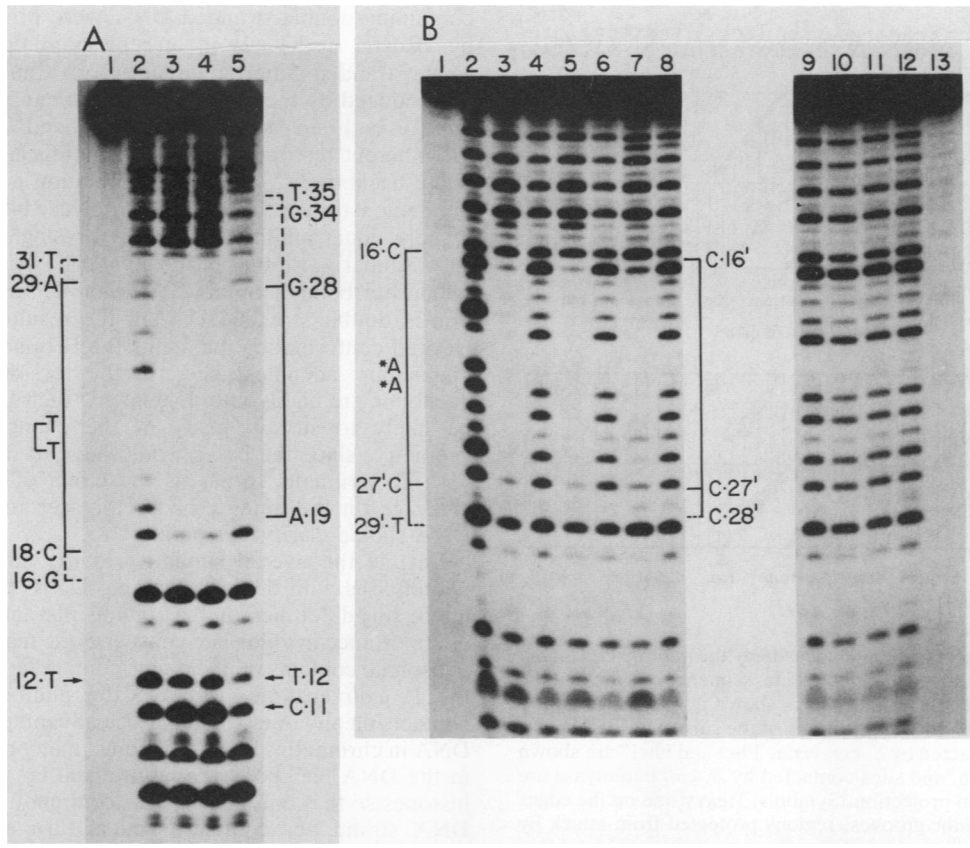

FIG. 6. DNase I footprint of photolyase. Large brackets on the left and right indicate areas protected by yeast photolyase (left) or *E. coli* photolyase (right) from digestion by DNase I. Numbering of bases in the sequence is as in Fig. 2. (A) Top strand. Bracketed T's indicate the position of the dimer. All lanes contain unique dimer substrate. Lanes: 1, substrate alone; 2, substrate treated with DNase I; 3 to 5, as lane 2 except that the substrate was incubated with Phr1, Phr1*, and *E. coli* photolyase, respectively, before addition of DNase I. (B) Bottom strand. Starred A's indicate the position opposite the dimer. Lanes: 1, unique dimer substrate only; 2, unique dimer substrate treated with DNase I; 3, as lane 2 except incubated with Phr1 before addition of DNase I; 4, as lane 3 except that the substrate-Phr1 complexes were exposed to photoreactivating light before addition of DNase I; 5 to 8, as lanes 3 and 4 except with Phr1* (lanes 5 and 6) and *E. coli* photolyase (lanes 7 and 8); 9 to 12, as lanes 2, 3, 5, and 7, respectively, except with nondimer DNA; 12, nondimer DNA digested with DNase I only; 13, nondimer DNA only.

binding proteins in vivo. The same phosphate and major groove contacts have been observed when photolyase from the archaebacterium *M. thermoautotrophicum* is bound to dimer-containing DNA (19a), indicating that this common recognition motif is conserved in all three kingdoms.

The sites of the common contacts made by the yeast and *E. coli* enzymes suggest a specific location for the enzymes when they bind to dimer-containing DNA. For the sake of discussion, we will assume that the structure of dimer-containing DNA is similar to the model proposed by Pearlman et al. (24). The primary features of this model are that dimer formation causes double-stranded B-DNA to unwind by 20° over a region of approximately 10 bp and to bend 27° into the major groove; H-bonding interactions between the dimerized pyrimidines and their base-pair partners remain and force the complementary bases into a nonplanar configuration. Both photolyases are in intimate contact with a 6- to 8-bp region symmetrically disposed around the dimer. Within this region, virtually every nucleotide on the dimer-containing strand, as well as three or four nucleotides on the nondimer strand, interacts with or is in close proximity to the enzymes (Fig. 7). Thus, the region of most extensive interaction corresponds precisely to the proposed region of maximal underwinding and compensatory overwinding of the helix (24). Backbone contacts are apparent at the first phosphate 5′ to the dimer and three to four phosphates 3′ to the dimer on the dimer-containing strand as well as at a single phosphate on the nondimer strand located across the minor groove from the 5′ and intradimer phosphate. Base nitrogens located in the major groove both 5′ and 3′ to the dimer are in close proximity to the enzymes, and interaction with the second nucleotide 3′ to the dimer contributes significantly to the binding strength or specificity. The enzymes also appear to lie in close proximity to the A's opposite the T's in the dimer, although only in the case of the yeast enzyme does interaction with one of these bases (or the attached sugar) contribute substantially to the stability of the enzyme-substrate complex. The locations of these contacts suggest that the photolyases approach the helix from the sugar-phosphate backbone of the dimer-containing strand, protrude into the major groove above (where they interact with the cyclobutane ring and with one or more bases) and into the minor groove below the backbone, and span the minor groove near the intradimer phosphodiester bond. In addition, removal of any of several bases 5′ or 3′ to the 6- to 8-bp core reduces binding. At present, it is not clear whether inhibition results from the loss of specific contacts that stabilize the enzyme-substrate complex or whether base

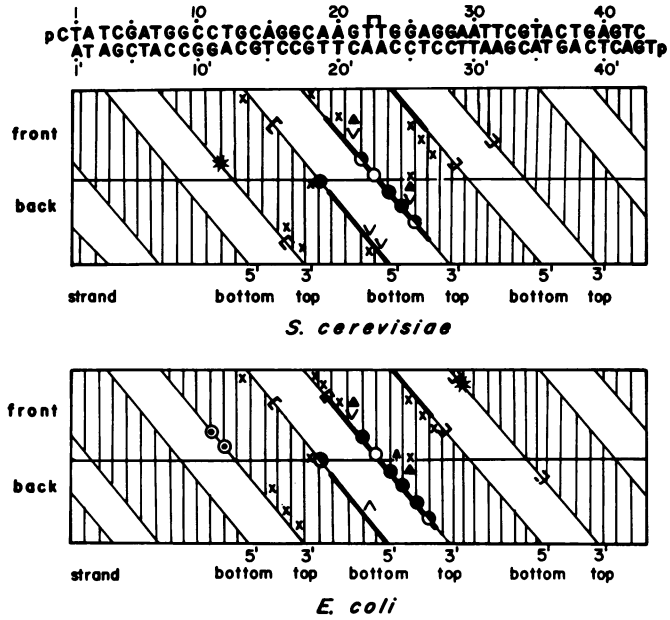

FIG. 7. Summary of the contacts made by the photolyases on the unique dimer substrate. The nucleotide sequence of the unique dimer substrate, with the dimer (⊓), is shown above planar representations of the cylindrical projections of the substrate (10.5 bp per turn [51]); sites contacted by *S. cerevisiae* Phr1 and Phr1* are shown on the top projection, and sites contacted by *E. coli* photolyase are shown on the bottom projection. Symbols: Heavy line on the edges of the major and minor grooves, regions protected from attack by MPE-FeII; ○, intradimer phosphate; ●, phosphate at which ethylation interfered strongly with binding; ○, phosphate at which ethylation interfered moderately with binding; V, base at which protein binding inhibited methylation; ↑, base at which protein binding enhanced methylation; ▲, base at which methylation inhibited protein binding; ×, base implicated in binding by the missing-contact experiments: [and], limits of regions protected from DNase I attack when photolyase was bound; *, phosphodiester bonds that became hypersensitive to DNase I when photolyase was bound; ⊙, phosphodiester bonds protected from DNase I outside the region of continuous protection.

removal induces a conformational change in the structure of the DNA that interferes with binding. In either case, the fact that these bases occupy the same face of the helix as does the cyclobutane ring and lie above and below the phosphate contacts on the dimer-containing strand is consistent with the proposed binding model.

If the distortion of the phosphodiester backbone induced by the dimer is indeed responsible for appropriate positioning of many of the groups on DNA that interact with the photolyases, two additional observations must be explained: (i) both yeast and *E. coli* photolyases also bind to single-stranded DNA containing pyrimidine dimers (41, 43; Sancar and Smith, unpublished observation); (ii) conditions that might be expected to relieve the distortion, namely, cleavage of the phosphodiester bond linking the dimerized nucleotides or cleavage of the glycosylic bond linking the 5′ pyrimidine to the sugar-phosphate backbone (12, 20, 53; this work), do not abolish photolyase binding. We believe that the explanation of these seemingly contradictory observations lies in the relative stability of the conformation induced in DNA by the dimer and that most of the contacts crucial for photolyase binding lie on the dimer-containing strand. Many of the altered torsion angles predicted in the model of dimer-containing double-stranded DNA were originally observed by Broyde et al. (2) in an energy-minimized model of single-stranded dimer-containing DNA; thus, the conformation induced by the dimer may be the energetically favored one for both single- and double-stranded DNA because of the inherent restriction of bond rotation in the sugar-phosphate backbone (28). This interpretation is consistent with our demonstration that *E. coli* photolyase binds with approximately equal affinity to double- or single-stranded DNA (41). Similarly, rupture of the glycosylic or intradimer phosphodiester bonds may not relieve the dimer-induced distortion in double-stranded DNA if the resulting energetically favored conformation maintains the H bonds with the complementary adenines; because the torsion angles in the backbone are highly interdependent, such H bonding would be likely to sustain many of the changes in the helix geometry, since the bases would have to remain nonplanar (24). Experiments to assess the effect of glycosylic bond cleavage on the binding of photolyases to single-stranded DNA should clarify this point.

Despite the overall similarity in the interactions of the photolyases with dimer-containing DNA, there are several interesting differences in the binding interactions that may be of importance in vivo. The yeast enzyme makes fewer strong phosphate contacts on the dimer-containing strand than does the *E. coli* enzyme. Limiting the number of phosphate contacts on any one strand may be advantageous for binding DNA in chromatin. In nucleosomes, many of the phosphates in the DNA backbone are neutralized by interactions with histones so that only four to five contiguous phosphates per DNA strand per complete helical turn are available for electrostatic interactions (22). The relatively small number of required phosphate contacts may permit yeast photolyase to repair dimers in vivo with minimal disruption of the nucleosomal structure. The results reported in this and the accompanying paper (37) also have important implications for the as yet unknown mechanism of nucleotide excision repair in *S. cerevisiae* (7, 49). Phr1 stimulates nucleotide excision repair in vivo in yeast cells (37), probably via direct interaction between the repair enzymes at the dimer site, suggesting that both enzymes must be able to bind simultaneously. This requirement would appear to rule out a pyrimidine dimer glycosylase-apyrimidinic endonuclease, similar to that isolated from phage T4 or *Micrococcus luteus*, as the enzyme responsible for the initial incision event because these enzymes are inhibited in vitro by binding of *E. coli* photolyase (30). Weinfeld et al. (52) have proposed that in human cells the initial incision occurs at the intradimer phosphodiester bond. Although we have not detected interaction between Phr1 and this bond, the intimate association of Phr1 with phosphates on either side of the dimer, as well as with the major groove above and the minor groove below, would likely preclude approach to this phosphate by another protein, thereby eliminating this model for nucleotide excision repair in yeast cells. Instead, our data are most consistent with a mode of excision repair in which the site(s) of incision is removed several base pairs from the lesion; the minimum distance from the dimer to the incision is delimited by the core region interacting with photolyase, that is, three to four phosphodiester bonds on each side of the dimer.

ACKNOWLEDGMENT

This work was supported by Public Health Service grant GM35123 from the National Institutes of Health.

LITERATURE CITED

1. **Banerjee, S. K. R. B. Christensen, C. W. Lawrence, and J. E. LeClerc.** 1988. Frequency and spectrum of mutations produced by a single cis-syn thymine-thymine cyclobutane dimer in a single-stranded vector. Proc. Natl. Acad. Sci. USA **85**:8141–8145.
2. **Broyde, S., S. Stellman, and B. Hingerty.** 1980. DNA backbone conformation in cis-syn pyrimidine[]pyrimidine cyclobutane dimers. Biopolymers **19**:1695–1701.
3. **Brunelle, A., and R. F. Schleif.** 1987. Missing contact probing of DNA-protein interactions. Proc. Natl. Acad. Sci. USA **84**: 6673–6676.
4. **Eker, A. P. M., R. H. Dekker, and W. Berends.** 1981. Photoreactivating enzyme from *Streptomyces griseus*. IV. On the nature of the chromophoric cofactor in *Streptomyces griseus* photoreactivating enzyme. Photochem. Photobiol. **33**:65–72.
5. **Eker, A. P. M., J. K. C. Hessels, and R. H. Dekker.** 1986. Photoreactivating enzyme from *Streptomyces griseus*. VI. Action spectrum and kinetics of photoreactivation. Photochem. Photobiol. **44**:197–205.
6. **Eker, A. P. M., J. K. C. Hessels, and J. van de Velde.** 1988. Photoreactivating enzyme from the green algae *Scendesmus acutus*. Evidence for the presence of two different flavin chromophores. Biochemistry **27**:1758–1765.
7. **Ferguson, L. R., and B. S. Cox.** 1974. Excision of bases accompanying the excision of dimers from DNA of UV-irradiated yeast. Mol. Gen. Genet. **135**:87–90.
8. **Fisher, G. J., and H. E. Johns.** 1976. Pyrimidine photodimers, p. 225–294. *In* S. Y. Wang (ed.), Photochemistry and photobiology of nucleic acids, vol. 1. Academic Press, Inc., New York.
9. **Fried, M., and D. M. Crothers.** 1981. Equilibria and kinetics of *lac* repressor-operator interactions by polyacrylamide gel electrophoresis. Nucleic Acids Res. **9**:6505–6525.
10. **Galas, D., and A. Schmitz.** 1978. DNase footprinting: a simple method for the detection of protein-DNA binding specificity. Nucleic Acids Res. **5**:3157–3170.
11. **Garner, M. M., and A. Revzin.** 1981. A gel electrophoresis method for quantifying the binding of proteins to specific DNA regions: application to components of the *Escherichia coli* lactose operon regulatory system. Nucleic Acids Res. **9**:3047–3060.
12. **Grafstrom, R. H., L. Park, and L. Grossman.** 1982. Enzymatic repair of pyrimidine dimer-containing DNA. A 5′ dimer DNA glycosylase: 3′-apyrimidinic endonuclease mechanism from *Micrococcus luteus*. J. Biol. Chem. **257**:13465–13474.
13. **Harm, H.** 1976. Repair of UV-irradiated biological systems: photoreactivation, p. 219–263. *In* S. Y. Wang (ed.), Photochemistry and photobiology of nucleic acids, vol. 1. Academic Press, Inc., New York.
14. **Harm, W., and B. Hillebrandt.** 1962. A nonphotoreactivable mutant of *E. coli* B. Photochem. Photobiol. **1**:271–272.
15. **Hertzberg, R. P., and P. B. Dervan.** 1984. Cleavage of DNA with methidiumpropyl-EDTA-Iron(II): reaction conditions and product analyses. Biochemistry **23**:3934–3945.
16. **Husain, I., and A. Sancar.** 1987. Binding of *E. coli* photolyase to a defined substrate containing a single T<>T dimer. Nucleic Acids Res. **15**:1109–1120.
17. **Husain, I., G. B. Sancar, S. R. Holbrook, and A. Sancar.** 1987. Mechanism of damage recognition by *Escherichia coli* DNA photolyase. J. Biol. Chem. **262**:13188–13197.
18. **Johnson, J. L., S. Hamm-Alvarez, G. Payne, G. B. Sancar, K. V. Rajagopalan, and A. Sancar.** 1988. Identification of the second chromophore of *Escherichia coli* and yeast DNA photolyase as 5,10-methenyltetrahydrofolate. Proc. Natl. Acad. Sci. USA **85**:2046–2050.
19. **Jorns, M. S., G. B. Sancar, and A. Sancar.** 1985. Identification of oligodeoxythymidylates as new simple substrates for *Escherichia coli* DNA photolyase and their use in a rapid spectrophotometric enzyme assay. Biochemistry **24**:1856–1861.

19a. **Kiener, A., I. Husain, A. Sancar, and C. Walsh.** 1989. Purification and properties of *Methanobacterium thermoautotrophicum* DNA photolyase. J. Biol. Chem. **264**:13880–13887.

20. **Liuzzi, M., M. Weinfeld, and M. Paterson.** 1987. Selective inhibition by methoxyamine of the apurinic/apyrimidinic endonuclease activity associated with pyrimidine dimer-DNA glycosylases from *Micrococcus luteus* and bacteriophage T4. Biochemistry **26**:3315–3321.
21. **Maxam, A. M., and W. Gilbert.** 1980. Sequencing end-labeled DNA with base-specific chemical cleavages. Methods Enzymol. **65**:499–560.
22. **Mirzabekov, A., and A. Rich.** 1979. Asymmetric lateral distribution of unshielded phosphate groups in nucleosomal DNA and its role in DNA bending. Proc. Natl. Acad. Sci. USA **76**:1118–1121.
23. **Myles, G. M., B. Van Houten, and A. Sancar.** 1987. Utilization of DNA photolyase, pyrimidine dimer endonucleases, and alkali hydrolysis in the analysis of aberrant ABC excinuclease incisions adjacent to UV-induced DNA photoproducts. Nucleic Acids Res. **15**:1227–1244.
24. **Pearlman, D. A., S. R. Holbrook, D. H. Pirkle, and S.-H. Kim.** 1985. Molecular models for DNA damaged by photoreaction. Science **227**:1304–1308.
25. **Rupert, C. S.** 1962. Photoenzymatic repair of ultraviolet damage in DNA. I. Kinetics of the reaction. J. Gen. Physiol. **45**:703–724.
26. **Rupert, C. S.** 1962. Photoenzymatic repair of ultraviolet damage in DNA. II. Formation of the enzyme-substrate complex. J. Gen. Physiol. **45**:725–741.
27. **Rupert, C. S., S. H. Goodgal, and R. M. Herriott.** 1958. Photoreactivation *in vitro* of ultraviolet inactivated *Hemophilus influenza* transforming factor. J. Gen. Physiol. **41**:451–471.
28. **Saenger, W.** 1984. Principles of nucleic acid structure. Springer-Verlag, New York.
29. **Saito, N., and H. Werbin.** 1970. Purification of a blue-green algal deoxyribonucleic acid photoreactivating enzyme. An enzyme requiring light as a physical cofactor to perform its catalytic function. Biochemistry **9**:2610–2620.
30. **Sancar, A., K. A. Franklin, and G. B. Sancar.** 1984. *Escherichia coli* DNA photolyase stimulates UvrABC excision nuclease *in vitro*. Proc. Natl. Acad. Sci. USA **81**:7397–7401.
31. **Sancar, A., and W. D. Rupp.** 1983. A novel repair enzyme: UVRABC excision nuclease of *Escherichia coli* cuts a DNA strand on both sides of the damaged region. Cell **33**:249–260.
32. **Sancar, A., and G. B. Sancar.** 1984. *Escherichia coli* DNA photolyase is a flavoprotein. J. Mol. Biol. **172**:223–227.
33. **Sancar, A., and G. B. Sancar.** 1988. DNA repair enzymes. Annu. Rev. Biochem. **57**:29–67.
34. **Sancar, A., F. W. Smith, and G. B. Sancar.** 1984. Purification of *Escherichia coli* DNA photolyase. J. Biol. Chem. **259**:6028–6032.
35. **Sancar, G. B.** 1985. Sequence of the *Saccharomyces cerevisiae PHR1* gene and homology of the Phr1 photolyase to *E. coli* photolyase. Nucleic Acids Res. **13**:8231–8246.
36. **Sancar, G. B., and A. Sancar.** 1987. Structure and function of DNA photolyases. Trends Biochem. Sci. **12**:259–261.
37. **Sancar, G. B., and F. W. Smith.** 1989. Interactions between yeast photolyase and nucleotide excision repair proteins in *Saccharomyces cerevisiae* and *Escherichia coli*. Mol. Cell. Biol. **9**:4767–4776.
38. **Sancar, G. B., F. W. Smith, and P. F. Heelis.** 1987. Purification of the yeast *PHR1* photolyase from an *Escherichia coli* overproducing strain and characterization of the intrinsic chromophores of the enzyme. J. Biol. Chem. **262**:15457–15465.
39. **Sancar, G. B., F. W. Smith, M. C. Lorence, C. S. Rupert, and A. Sancar.** 1984. Sequences of the *E. coli* photolyase gene and protein. J. Biol. Chem. **259**:6033–6038.
40. **Sancar, G. B., F. W. Smith, R. Reid, G. Payne, M. Levy, and A. Sancar.** 1987. Action mechanism of *Escherichia coli* DNA photolyase. I. Formation of the enzyme-substrate complex. J. Biol. Chem. **262**:478–485.
41. **Sancar, G. B., F. W. Smith, and A. Sancar.** 1985. Binding of *Escherichia coli* DNA photolyase to UV-irradiated DNA. Biochemistry **24**:1849–1855.
42. **Setlow, J. K.** 1964. Effects of UV on DNA: correlations among biological changes, physical changes, and repair mechanisms. Photochem. Photobiol. **3**:405–413.
43. **Setlow, J. K., and F. J. Bollum.** 1968. The minimum size of the

substrate for yeast photoreactivating enzyme. Biochim. Biophys. Acta **157**:233–237.
44. **Setlow, R. B., and W. L. Carrier.** 1966. Pyrimidine dimers in ultraviolet-irradiated DNAs. J. Mol. Biol. **17**:237–254.
45. **Siebenlist, U., and W. Gilbert.** 1980. Contacts between *Escherichia coli* RNA polymerase and an early promoter of phage T7. Proc. Natl. Acad. Sci. USA **77**:122–126.
46. **Siebenlist, U., R. B. Simpson, and W. Gilbert.** 1980. *E. coli* RNA polymerase interacts homologously with two different promoters. Cell **20**:269–281.
47. **Suck, D., and C. Oefner.** 1986. Structure of DNaseI at 2.0 Å resolution suggests a mechanism for binding to and cutting DNA. Nature (London) **321**:620–625.
48. **Sutherland, B. M.** 1981. Photoreactivating enzymes, p. 481–515. *In* P. D. Boyer (ed.), The enzymes, vol. 14. Academic Press, Inc., New York.
49. **Unrau, P., R. Wheatcroft, and B. S. Cob.** 1971. The excision of pyrimidine dimers from DNA of ultraviolet irradiated yeast. Mol. Gen. Genet. **354**:359–362.
50. **Van Dyke, M. W., and P. B. Dervan.** 1983. Methidiumpropyl-EDTA · Fe(II) and DNaseI footprinting report different small molecule binding site sizes on DNA. Nucleic Acids Res. **11**: 5555–5567.
51. **Wang, J. C.** 1979. Helical repeats of DNA in solution. Proc. Natl. Acad. Sci. USA **76**:200–203.
52. **Weinfeld, M., N. E. Gentner, L. D. Johnson, and M. C. Paterson.** 1986. Photoreversal-dependent release of thymidine and thymidine monophosphate from pyrimidine-dimer containing DNA excision fragments isolated from ultraviolet-damaged human fibroblasts. Biochemistry **25**:2656–2664.
53. **Weinfeld, M., and M. C. Paterson.** 1988. DNA cyclobutane dimers with a cleaved internal phosphodiester bond can be photoenzymatically reversed by *Escherichia coli* PhrB photolyase. Nucleic Acids Res. **16**:5693.
54. **Yamamoto, K., Y. Fujiwara, and H. Shinagawa.** 1984. A multicopy *phr*-plasmid increases the ultraviolet resistance of a *recA* strain of *Escherichia coli*. Mutat. Res. **131**:11–18.
55. **Yasui, A., and S. A. Langeveld.** 1985. Homology between the photoreactivation genes of *Saccharomyces cerevisiae* and *Escherichia coli*. Gene **36**:349–355.
56. **Yasui, A., M. Takao, A. Oikawa, A. Kiener, C. T. Walsh, and A. P. M. Eker.** 1988. Cloning and characterization of a photolyase gene from the cyanobacterium *Anacystis nidulans*. Nucleic Acids Res. **16**:4447–4463.